Title
POLARIZATION OF SILVER NUCLEI IN METALLIC IRON AND NICKEL

Authors
Westenbarger, G.A.
Shirley, D.A.

Publication Date
1964-06-01

UCRL-11505

University of California

Ernest O. Lawrence Radiation Laboratory

POLARIZATION OF SILVER NUCLEI IN METALLIC IRON AND NICKEL

Berkeley, California

DISCLAIMER

For Phys. Rev.

UCRL-11505

UNIVERSITY OF CALIFORNIA

Lawrence Radiation Laboratory
Berkeley, California

AEC Contract No. W-7405-eng-48

POLARIZATION OF SILVER NUCLEI IN METALLIC IRON AND NICKEL

G. A. Westenbarger and D. A. Shirley

June 1964

POLARIZATION OF SILVER NUCLEI IN METALLIC IRON AND NICKEL

G. A. Westenbarger and D. A. Shirley

Department of Chemistry and
Lawrence Radiation Laboratory
University of California
Berkeley, California

June 1964

ABSTRACT

Nuclei of Ag^{104} and Ag^{110m} were polarized at temperatures between 0.0105° K and 0.97° K, employing the large hyperfine magnetic fields induced at the nuclei of silver atoms dissolved in iron and in nickel. The temperature and angular dependences of γ-ray angular distributions were used to determine the magnitudes of the hyperfine structure constants. Nonconservation of parity in beta decay was used to determine the signs of the internal fields, using germanium detectors to count positrons from Ag^{104} and electrons from Ag^{110m}. The hyperfine fields were found to be negative in both iron and nickel. Analysis of the γ-ray data on one-hour Ag^{104} yielded approximate values for the internal fields: H_i(Ag in Fe) = - 350 ± 100 kgauss, H_i(Ag in Ni) = - 108 ± 30 kgauss. Cobalt-60 γ-ray thermometry was used, and the problems of thermometry at 0.01° K are discussed.

Nuclear spins of four levels in Cd^{110} were determined unambigously, confirming earlier work, which was re-interpreted where necessary. The energy levels (spins) are 2162 keV (3+), 2219 keV (4+), 2479 keV (6+), 2926 (5+). The 1384 keV γ ray in Cd^{110} was found to be (91.7 ± 2.8)% magnetic dipole and (8.3 ± 2.8)% electric quadrupole. The 1505 keV γ ray was (78.9 ± 4.8)% magnetic dipole and (21.1 ± 4.8)% electric quadrupole. An approximate value of + 2.9 ± 1.3 nm was determined for the nuclear moment of Ag^{110m}.

I. INTRODUCTION

Since the discovery by Samoilov, Sklyarevskii, and Stepanov[1] that large hyperfine magnetic fields are induced at nuclei of atoms dissolved in iron, several such fields have been measured. No quantitative theory for these induced fields exists; in fact even an unambiguous qualitative understanding is not presently available. It seems important, therefore, to make systematic measurements of induced fields at nuclei of various elements throughout the periodic table, with emphasis on those systems that are most accessible to theoretical study. With this aim we have performed nuclear orientation experiments on silver atoms in iron and nickel lattices. This study complements measurements on the other group IB metals, copper [2,3] and gold.[4,5]

The theory and applicability of the technique are discussed in Section II. The apparatus is described in Section III. Section IV deals with the important subject of thermometry. In Section V nuclear results are derived, and in Section VI the induced magnetic fields at Ag nuclei in Fe and Ni are deduced.

II. THEORY OF THE MEASUREMENTS

The general theory of nuclear orientation has been formulated by several authors.[6-8] Only those parts of the theory that are applicable to the polarization of nuclei in ferromagnets are summarized here.

Polarization of nuclei in a ferromagnet arises through interaction of the nuclear magnetic dipole moment, $\vec{\mu}$, with a hyperfine magnetic field, $\vec{H}_i$. The sense and direction of $\vec{H}_i$ are fixed in space

by a small polarizing field, $\vec{H}_e$, applied externally. The orders of magnitude of $\vec{H}_i$ and $\vec{H}_e$ are 10^5-10^6 gauss and 10^3 gauss, respectively. Thus $\vec{H}_e$ establishes a quantization axis along the resultant field, $\vec{H}_r = \vec{H}_i + \vec{H}_e'$. Here $\vec{H}_e'$ is the external field modified in the usual way by the Lorentz field and the demagnetizing field. It is important to note that $\vec{H}_r$ need not be parallel or antiparallel to $\vec{H}_e$.

The Hamiltonian governing orientation of the spin system is

$$\mathcal{H} = -\vec{\mu} \cdot \vec{H}_r = - g\beta_N M H_r \quad . \tag{1}$$

Here g is the nuclear g-factor, β_N is the nuclear magneton, and M is the component of nuclear spin along the quantization axis. At equilibrium the spins are distributed according to the statistical population function

$$W(M) = Z^{-1} \exp (-g\beta_N M H_r/kT) \quad , \tag{2}$$

where Z is the partition function. Substantial nuclear orientation occurs when $g\beta_N H_r/kT$ is of the order of unity or larger. For g = 1 this requires that H_r/T be 2.8×10^7 gauss/degree. Thus temperatures of the order of 10^{-2} degrees Kelvin are required for orientation even in most of the large internal fields available in ferromagnets.[9]

The degree of orientation is most conveniently given by the usual statistical tensors[8]

$$B_k = (2I + 1)^{1/2} \sum_m (-)^{I-M} C(IIk;M-M) W(M) \quad , \tag{3}$$

and the angular distribution of radiation following the decay of oriented nuclei can be written

$$W(\theta) = \sum_{k=0}^{\lambda} B_k U_k F_k P_k (\cos\theta) \quad . \qquad (4)$$

Here θ is the angle between the propagation direction of the radiation and the quantization axis. The functions U_k and F_k are discussed by Blin-Stoyle and Grace.[8] Angular momentum triangle conditions set an upper limit λ on the rank of nonvanishing tensors. For the work discussed here no radiation quanta carried more than two units of angular momentum from the nucleus; therefore λ was 4. Because parity is conserved in electromagnetic interactions, only the $K = 0,2,4$ terms contributed to the angular distribution of gamma radiation. Parity is not conserved in beta decay, and the $k = 0,1$ terms were important in the angular distributions of beta particles. Higher k gave no contributions to the beta-particle distributions from Ag^{104} and Ag^{110m} because[10] the transitions were allowed.[11]

A careful determination of the temperature dependence of $B_2U_2F_2$, together with knowledge of U_2F_2, yields $B_2(T)$ directly. By combining $B_2(T)$ with Eqs. (2) and (3), one obtains $|\mu H_r|$. From γ-ray directional distributions alone one cannot obtain the sign of this product, because there are no odd k terms in Eq. (4). (γ-ray circular polarization measurements do yield the sign.) If enough is known about the observed beta transition, a determination of the sign of the "forward-backward" beta asymmetry yields the sign of the μH_r product. For a pure Gamow-Teller transition (Ag^{104}) with I(initial) = I(final) + 1, the angular distribution is given by[6,8]

$$W(\theta,e^{\pm}) = 1 \pm \left(\frac{I+1}{3I}\right)^{1/2} \left(\frac{v}{c}\right) B_1 \cos\theta \quad . \qquad (5)$$

For $\Delta I = 0$ and a Gamow-Teller transition, the distribution is given by

$$W(\theta,e^{\pm}) = 1 \pm \left|\frac{1}{3I(I+1)}\right|^{1/2} \left(\frac{v}{c}\right) B_1 \cos\theta \quad . \qquad (6)$$

In both (5) and (6) v is the electron velocity and θ is taken as zero in the positive sense along the quantization axis.

III. APPARATUS

It seems very probable that the orientation, by induced hyperfine fields, of nuclei of atoms dissolved in iron and other magnetic lattices will be exploited considerably in the near future. The cryogenic techniques required for these experiments are somewhat demanding and not generally known. Several features of our apparatus, including its ability to cool radioactive specimens to 0.0105° K and to keep them in this temperature range for hours, are unique. Thus we describe the essential points of this apparatus below.

The helium bath could be pumped to 0.97° K by the use of a 1250 CFM mechanical booster pump. At this temperature the equilibrium adsorption pressure of He^4 heat-exchange gas is very low and a cryostat pressure of 10^{-6} mm Hg could be obtained by only a few minutes of pumping. The cryostat was made of glass to facilitate inductance measurements and to provide a clean surface; it was joined to the vacuum system by a Housekeeper seal and soft solder. Care was taken to make the entire exchange-gas vacuum system as clean as possible, using welded stainless-steel tubing wherever feasible.

The iron-alloy sample, of approximate dimensions 4 mm × 2 mm × 0.1 mm, was soft-soldered to a laminated fin assembly consisting of 25 pieces of 0.005" Cu foil, silver-soldered together at the top. The foils were cut with a protrusion to support the sample at the top end; the bottom end of each foil made contact with a "chrome alum-glycerine" slurry. The slurry was prepared by stirring powdered chromium potassium sulfate with a 1:1 by volume mixture of a saturated aqueous solution of chromium potassium sulfate and glycerine. The usual proportions were 12 g. of salt to 5 g. of 1:1 mixture, but the consistency of the slurry determined the exact composition in each case. The slurry was carefully spread onto both sides of each fin and the assembly was placed into a glass container which was in turn suspended by spring-loaded nylon threads in the cryostat vacuum space. The protrusion holding the sample was inserted into (but did not touch) a 3/8" long by 1/2" O.D. by 3/8" I.D. niobium metal tube. At 1° K this superconducting tube trapped over 2000 gauss during the demagnetization, thus polarizing the sample. The total contact area of copper fins and slurry was 800 cm^2, and new slurry was made for each run.

IV. THERMOMETRY

Thermometry in the $10^{-2}{}^{\circ}$ K temperature range is in a very primitive state. Most "magnetic temperature scales" for paramagnetic salts yield absolute temperatures with quoted accuracies of only about 10%, and various evidence obtained by nuclear orientation measurements in this laboratory indicates that these estimated errors are by no means too large. Thus, while a $T\text{-}T^*$ correlation for chrome alum is available, it would be very unattractive to base quantitative results on this correlation.

There are additional objections against using only magnetic thermometry. Thermal equilibrium between sample and slurry is not possible because an appreciable fraction of the total heat leak (including radioactive heating) comes in through the sample and fin assembly. The shape of the paramagnetic slurry, partitioned by the copper fins, was such as to preclude an exact demagnetization-factor correction. Finally the instability of chrome alum itself casts doubt on magnetic thermometry employing it.

We elected to measure temperatures "internally" by incorporating Co^{60} into the sample and using the angular distributions of the 1.173 and 1.333 MeV γ rays following the decay of oriented Co^{60} to determine the temperature. This procedure is thermodynamically imperfect in the sense of not being completely empirical. It is, however, valid to the extent that the Hamiltonian governing the orientation of Co^{60} nuclei in iron is known. This Hamiltonian has the form of Eq. (1), with H_i = - 289.7 kgauss,[12] and H_e = + 2.3 kgauss. The nuclear moment of Co^{60} has the value + 3.80 nm.[13] The absolute temperature is contained implicitly in the formalism of Section II.

Gamma-ray thermometry has been used before,[14-16] usually to compare nuclear moments. It should be emphasized that such a comparison is possible only if the temperature of the specimen is homogeneous and if the spin Hamiltonian of the "standard" isotope and the <u>form</u> of the spin Hamiltonian of the isotope to be investigated are known.

If the appropriate criteria have been met, we believe that it is both theoretically valid and experimentally feasible to use nuclear orientation to establish a primary temperature scale in the 0.01° K range, with an absolute accuracy as high as 1%. This applies both to

experiments of the type reported here and to ionic crystals, and it would constitute a tenfold improvement over the best accuracy presently available.

Figure 1 shows a "warming curve" for a well-insulated chrome alum slurry and fin assembly. The susceptibility maximum accompanying the Curie point of chrome alum (at 0.0115° K)[17] is clearly visible, and it comes one hour after demagnetization. In the experiments reported here this type of warming curve served as a criterion of good apparatus performance.

Temperatures obtained from the Co^{60} γ-ray thermometer and the magnetic thermometer are compared in Fig. 2. The Co^{60} γ-ray intensity for the run that was used in Fig. 1 and that appeared in Fig. 2 is plotted against time in Fig. 3. The lowest γ-ray temperature was 0.0105° K, substantially below the accepted Curie point of 0.0115° K. However, the sample temperature was 0.0115° K fifty minutes after demagnetization, when the salt in the slurry was at the susceptibility maximum. If the salt and sample were in thermal equilibrium at this point, this agreement would support the established Curie point. We can say with confidence that the Curie point of chrome alum is no higher than 0.0115° K.

In the early stages of this work a value of -80 kgauss for the internal field of Co in Ni was used and the nickel data did not agree with the iron data. The Co in Ni thermometer consistently suggested that temperatures in the $1/T \cong 120$ range were being reached. The -80 kgauss internal field had been obtained by a rather questionable extrapolation of heat capacity data.[18] After many experiments had established our confidence in the Co^{60} thermometer, we abandoned this internal field value in favor of a value of -120 kgauss which we determined and were prepared to report. An NMR measurement then became available,[19]

H_i = - 112.7 kgauss at 27.4° C. This may be corrected to -123 kgauss at 0° K, in very good agreement with our result.

V. NUCLEAR RESULTS

The energy-level scheme of Cd^{110}, as deduced from the decay of Ag^{110m}, is shown in Fig. 4. Most of the information given there was taken from electron and γ-ray spectroscopy measurements and angular correlation work in the literature.[11,20-26] The nuclear orientation results that we report here serve to establish some spins uniquely, to confirm others, and (especially in conjunction with the angular correlation data) to determine multipolarity mixtures in mixed M1-E2 transitions with good accuracy.

The approach used in analyzing the data was to determine $B_2U_2F_2$ (the coefficient of P_2 in Eq. (4)) with high precision for each γ ray, where possible. The spectrum is complex (Fig. 5), and several γ rays are unresolved. Fortunately the energies and approximate relative intensities are available.[21,24,26] The analysis was necessarily implicit, and the $B_4U_4F_4$ term, which was always small, was treated as a correction. The background correction for lower energy γ rays, which arises largely from Compton scattering of higher energy γ rays, presents a very difficult problem. One cannot, for example, assume that this background is isotropic, as it certainly isn't. The anisotropy of Compton-scattered radiation isn't equal to that of the corresponding photopeak, either (as it would very nearly be if scattering occurred only in the NaI crystal); in fact it may even have the opposite sign, because of the γ ray polarization.[27] An estimate of the experimental background anisotropy may be obtained from Fig. 6, in which the intensity

at $\theta = 0$ and $T = 0.01^{\circ}$ K is plotted against photon energy. The photopeaks that will yield the most reliable anisotropies are those at the highest energies, in this case the 885, 937, 1384, and 1505 keV peaks.

In Table I the average values of $B_2U_2F_2$ for several peaks are set out. These were obtained by averaging data for each peak from several runs for which the reciprocal temperatures were near the average value of 90 deg.$^{-1}$. We note that the values of $B_2U_2F_2$ have relative precisions in some cases far better than their absolute accuracies. Thus the figure $1/T = 90$ deg.$^{-1}$ is a nominal value, known to no better than 2%. We discuss the peaks separately below.

The 885-keV peak. This γ ray is known to have E2 multipolarity and has a well-established position in the decay scheme. We use it as our internal standard of comparison to determine F_2's for the other γ rays (leading to a 5% correction noted at the end of this section). For the spin-multipolarity combination 4(E2)2, we have $F_2(885) = -0.448$. The U_2 for this transition can be calculated from the spins, multipolarities, and relative intensities of preceeding transitions (although this is a "bootstrap" operation in that the resulting quantities will be used to determine these spins and multipolarities, U_2 is a slowly varying function of these parameters, and it is not possible, in this case, to converge on a spurious solution by iteration). By this procedure we find $U_2(885)=0.763 \pm 0.034$. Comparison with Table I yields $B_2 = +0.95 \pm 0.05$. The quoted error arises from uncertainties the temperature scale, background corrections, and the error in the determination of $U_2(885)$. At the end of this Section this B_2 will be revised downward by 5% to bring it into better agreement with other angular distribution data.

The "658-keV" peak. This peak includes the 620 and 677 keV γ rays as well as its main component, the 658-keV γ ray. The value of $B_2U_2F_2$ for the 658-keV γ ray should, from the decay scheme, be + 0.964 ± 0.041 times that of the 885-keV γ ray. From Table I, the ratio $B_2U_2F_2$ ("658 peak")/ $B_2U_2F_2$ (885) is in fact + 0.66 ± 0.02. This lower ratio must arise from contributions to the "658 peak" of the 620- and 677-keV γ rays, which must have values of $B_2U_2F_2$ quite different from that of the 658-keV γ ray. Detailed analysis gave the limits on $B_2U_2F_2$ (620) and $B_2U_2F_2$ (677) that are listed in Table I.

The 1384-keV peak. From Table I we find $U_2F_2(1384)/U_2F_2(885) = - 2.10 \pm 0.05$. For a pure Gamow-Teller transition from the 6+ state in Ag^{110m} to the 2925-keV level, we have $U_2 = + 0.97$. A 6+ spin and parity combination for this level is immediately ruled out by the sign of $B_2U_2F_2(1383)$. Thus we find

$$F_2^{L}(1384) = + 0.74 \pm 0.05 \quad ,$$

where "L" denotes last in a cascade.[28] The amplitude mixing ratio, δ(E2/M1), for this cascade is thus either $\delta^{L} = - 0.273 \pm 0.027$ or $\delta = - 2.21 \pm 0.15$. This latter possibility is easily ruled out by the angular correlation data, which are in reasonable agreement for the former value. Actually the quoted error limits for the various experiments do not quite overlap, but the errors quoted for the angular correlation data are too small, considering that little or no correction was made for interfering radiations for which the intensities were then unknown. The angular correlation results and the values of $F_2^{F}(1384)$ obtained from the available angular correlation data are

listed, along with the derived values of δ^F, in Table II. We note that by definition[28,29] $\delta^F = -\delta^L$. The data are all consistent with the 1384 keV transition being of (8.3 ± 2.8)% dipole and (91.7 ± 2.8)% quadrupole multipolarity and proceeding from a 5+ state at 2925 keV to a 4+ state at 1542 keV in Cd^{110}.

The 1505-keV peak. This peak is complex; it consists of γ rays at 1476, 1505, and 1561 keV, in relative intensities 5.5:14:1.3. The 1476 and 1561 keV transitions are "stretched" E2 transitions between states of known spins. Thus their angular distribution coefficients may be calculated.

Angular correlation data are available for two cascades involving the 1505-keV transition. Taylor and Frishen studied the 764-1505 keV cascade, finding $A_2 = -0.1627 \pm 0.0063$ and $A_4 = -0.0031 \pm 0.0098$. These results require $F_2^L(1505) = +0.79 \pm 0.03$, if no corrections are made for competing radiations. This F_2 should be revised slightly upward to account for inclusion of the 1476 keV γ ray in the correlation, both through the 744-1476 cascade and through the 764-687-1476 keV cascade. We cannot assess the corrections accurately because not enough information is available, but an estimate may be made from known relative intensities, spins, and multipolarities. After this correction, we find $F_2^L(1505) = +1.03 \pm 0.06$. After corrections for the angular distributions of the 1476- and 1561-keV γ rays, our nuclear orientation data give $F_2^L(1505) = +1.06 \pm 0.10$, in excellent agreement.

Angular correlation data are also available, for the 1505-658 keV cascade, in which the 1505-keV γ ray is first in cascade. The A_2's and derived values for $F_2^F(1505)$ are given in Table III. We conclude that all the data are consistent only with the 1505-keV transition being a

(78.9 ± 4.8)% M1 and (21.1 ± 4.8)% E2, proceeding from a 3+ state at 2162 keV to a 2+ state at 658 keV.

The 937-keV peak. The ratio $U_2F_2(937)/U_2F_2(885) = 0.957 \pm 0.031$ leads to $F_2(937) = -0.364 \pm 0.027$, based on $F_2(885) = -0.448$, $U_2(885) = +0.763 \pm 0.034$, and $U_2(2479) = +0.90 \pm 0.03$. This is slightly lower than the theoretical $F_2 = -0.402$ for a 6(Q)4 transition, but we regard the agreement as satisfactory. The other spin possibility of 5+ for the 2479-keV level, would require an F_2^L of -0.20 to be consistent with the angular correlation data.

The 706-keV peak. A large positive value for $F_2^L(706)$ was observed. An F_2^L of -0.420 would be required if this transition were 5(Q)3. Thus the spin of the 2219 keV level is not 3. A spin of 5 would require that the 744-keV transition be octupole, and would probably be accompanied by a beta branch from Ag^{110m}. Thus we conclude that the 2219-keV level has spin 4.

The above arguments lead to the spins indicated in Fig. 4 for the upper levels in Cd^{110}. These assignments are unambiguous and alternative assignments would require very different angular distributions, as discussed above. At the same time the derived F_2 coefficients for the three transitions for which accurate data are available are not in perfect agreement. Using the 885-keV transition as a standard, as we have above, our derived values for $F_2(937)$ and $F_2(1384)$ are, respectively, 9% and 12% lower than the best values from angular correlation, and the "probable error" intervals don't quite overlap. The choice of the 885-keV transition as a standard was somewhat arbitrary, and we have therefore corrected the empirical $B_2U_2F_2(885)$ upward by 5%, to obtain a most probable value, for the determination of hyperfine structure constants

in the next Section. This adjustment, which is within the possible error of the measurements, is entirely equivalent to taking the weighted average of the 885-, 937-, and 1384-keV data.

VI. HYPERFINE STRUCTURE AND INTERNAL FIELDS

(A) Magnitudes of the Hfs Constants for Ag^{110m}

From the above analysis enough was known to obtain quite consistent values of U_2F_2 for the peaks at 658, 885, 1384, and 1505 keV, especially considering the complexity of the spectrum. Samples of Ag^{110m} in iron and nickel were run, using Co^{60} as a thermometer. Values of $B_2(T)$ were obtained, using Eq. (2-4). These are compared with theoretical curves in Figs. 7 and 8. Only the absolute values, $|\mu H|$, could be derived from these data. These values are

$$|\mu H| = (10.0 \pm 0.07) \times 10^5 \text{nm gauss } (Ag^{110m} \text{ in Fe}) \quad ,$$

$$|\mu H| = (3.1 \pm 0.4) \times 10^5 \text{nm gauss } (Ag^{110m} \text{ in Ni}).$$

The solubility of Ag in Fe is reported[30] to be less than $2 \times 10^{-3}\%$. These experiments were run with concentrations of $10^{-3}\%$ and $0.5 \times 10^{-3}\%$ to test the possibility that the Ag was imcompletely dissolved. The results for these two concentrations were identical, indicating that the Ag present was all in solution in both cases (this of course implies nothing about the equilibrium solubility). Determination of the $B_4U_4F_4(885)$ product provides an independent test of whether the Ag atoms are in the Fe lattice. It is easily shown that, if only a fraction of the Ag^{110m} nuclei are oriented and contribute to

$B_2U_2F_2$, an anomalously large $B_4U_4F_4$ will be derived from the analysis (because an erroneously low hfs constant will be calculated). The actual $B_4U_4F_4(885)$ products indicate no such behavior (Fig. 9), and lend further support to our values for $|\mu H|$.

(B) Sign of μH for Ag^{110m}

Determination of the sign of μH by the use of parity nonconservation in beta decay is a straightforward process if enough is known about the beta decay. In the decay of Ag^{110m} only the 530-keV beta branch may be conveniently studied. We used germanium beta counters, which had been shown by Navarro[31] to give good resolution for electrons at 1° K, to study the asymmetry of the 530-keV beta branch from polarized Ag^{110m}.

This beta branch is almost entirely a Gamow-Teller transition; Daniel et al.[32] give $C_V M_F / C_A M_{GT} = 0.05 \pm 0.04$. For a pure 6+ to 6+ Gamow-Teller transition A- is -1/7, and we may write for the expected angular distribution of 511-keV electrons:

$$W(\theta) = 1 - 0.0775\, B_1(T) \cos\theta \quad ,$$

where θ is the angle between the polarizing field (vector) and the direction of the counter (from the source). For Ag^{110m} in Fe the γ ray data yield a hfs constant that implies $B_1 \sim 1.3$ at the lowest temperatures attainable. For Ag^{110m} in Ni this figure is $B_1 \sim 0.7$. Thus asymmetries of a few percent were expected in either case. Asymmetries were found, of ~11% in Fe and ~ 6% in Ni. In both cases the μH product was found to be negative. Measurements were made at several electron

energies and for $\theta = 0$ and π in each case. Neither the energy calibration nor the scattering properties of the source were of a quality to allow a precise measurement of the asymmetry but its sign was easily determined. Typical spectra are shown in Figs. 10 and 11.

There is independent evidence from atomic-beam measurements[33] that the magnetic moment of Ag^{110m} is large. The largest nuclear moments are always positive (because of the proton's orbital contribution); therefore the most probable interpretation of the negative μH products is that μ is positive and H negative. Negative internal fields were expected for these cases. The signs were determined directly as described below.

(C) The Hyperfine Structure of Ag^{104} in Iron

After the Ag^{110m} measurements were complete we did an experiment on 69-minute Ag^{104} in iron to determine the sign of the internal field directly. The spin and moment are known[34,35] to be $I = 5$ and $\mu = +4.0^{+0.2}_{-0.1}$ nm. This isomer decays[36] by positron emission to a 4+ state at 2270 keV in Pd^{104}. The angular distribution parameters may be calculated from the decay scheme. The $\beta+$ branches to the known 4+ states (Fig. 12) should be pure Gamow-Teller, and the 920-keV γ ray should be pure E2. The short lifetime precluded highly accurate measurements, but we were able to obtain some information about the internal field from the experiment. The Ag^{104} was prepared by a (p,n) reaction on Pd^{104}, and the alloy contained 5% Pd. This may affect the internal field at the Ag nuclei; it is probable that the error thus introduced is small compared to other errors in the experiment.

The γ-ray spectra for typical "cold" and "warm" counts are shown in Fig. 13. A large source of possible error is the background

correction for the 920 keV γ ray, which could be made only approximately in view of the incomplete knowledge of this decay. We can set extreme upper and lower limits on the internal field (Fig. 14) as follows: (a) The upper limit. The background under the 920-keV peak cannot be more than 43% of the total "warm" intensity, and the best estimate is 28 %. If the extreme value of 43% is used, and the correction is made, the internal field required to fit the data varies from 700 kgauss at 0.03° K to 450 kgauss at 0.015° K. We thus find that this latter value is an upper limit for the internal field. An independent check is the fact that the small $B_4U_4F_4$ coefficient of -0.04 ± 0.03 for this lowest temperature implies an internal field of 320 ± 130 kgauss. (b) The lower limit. If no background corrections whatever are made (or if the background is assumed to have the same angular distribution as the 920-keV peak), the fields required to fit the data fall between 300 and 400 kgauss. Taking into account all the possible sources of error, a field of 250 kgauss for Ag in Fe seems a conservative lower limit.

With these limits, we suggest 350 ± 100 kgauss as a tentative value for the magnitude of the hyperfine field at Ag nuclei in Fe. It follows from the above Ag^{110m} results that the corresponding value for Ag in Ni is 117 ± 33 kgauss. Because of experimental difficulties the Ag^{104} γ-ray experiments are intrinsically of low accuracy. Rather than trying to improve this accuracy slightly by further experiments in Ag^{104}, we prefer to determine the moment of Ag^{110m} by resonance methods and to obtain the internal fields by comparison of this moment with the hfs constants for Ag^{110m} in Fe and Ni. Such experiments are underway.

The main purpose of the Ag^{104} experiments was a sign determination of the hyperfine fields. This was easily done, with the results shown in Fig. 15. For a 5+ (β^+)4+ transition, the coefficient of cos θ

in Eq. (5) is positive; that is, positrons are preferentially emitted along the direction of the angular momentum vectors (i.e., along the polarization direction) of the parent nuclei. The higher intensity was observed with the small polarizing field at 180° from the counter direction. Thus the internal field must have oriented the nuclei antiparallel to the polarizing field. Since the nuclear moment is positive, it follows that the internal field was itself antiparallel to the external field, or negative. The tentative values for the internal fields now become

$$H_i = -(350 \pm 100) \text{ kgauss (Ag in Fe)},$$

$$H_i = -(108 \pm 30) \text{ kgauss (Ag in Ni)}.$$

It should be noted that the magnitudes of these fields are based on nuclear orientation experiments with an isotope of 1-hour half-life, in an iron-palladium alloy. More reliable (and more accurate) values await a determination of the magnetic moment of Ag^{110m}.

(D) Interpretation of the Internal Fields

The internal fields determined here can best be interpreted as part of a systematic discussion of induced internal fields. Such a discussion appears separately in the following paper. We note here that the field derived above for Ag in Fe is in good agreement with the value predicted[4] on the basis of the systematics, $H = -400$ kgauss. The quantitative agreement must not be taken too seriously, because neither value is very accurate. Still the sign is negative, as predicted, and we conclude that the systematic correlation has some predictive value.

FOOTNOTES AND REFERENCES

1. B. N. Samoilov, V. V. Sklyarevskii, and E. P. Stepanov, Zh. Eksptl. i Teoret. Fiz (USSR) 36, 644 (1959); Soviet Phys. JETP (English Transl.) 9, 448 (1959).

2. T. Kushida, A. H. Silver, Y. Koi, and A. Tsujimura, J. Appl. Phys. Suppl. 33, 1079 (1962).

3. K. Asayama, S. Kobayashi, and J. Itoh, J. Phys. Soc. Japan 18, 458 (1963).

4. R. W. Grant, Morton Kaplan, D. A. Keller, and D. A. Shirley, Phys. Rev. 133, A1062 (1964).

5. L. D. Roberts and J. O. Thomson, Phys. Rev. 129, 664 (1963).

6. W. J. Huiskamp and H. A. Tolhoek, Orientation of Atomic Nuclei at Low Temperatures III, in Progress in Low Temperature Physics III, ed. by C. J. Gorter (North-Holland Publishing Company, Amsterdam, 1961) p. 333.

7. H. A. Tolhoek and J. A. M. Cox, Physica 19, 101 (1953).

8. R. J. Blin-Stoyle and M. A. Grace, Oriented Nuclei, in Handbuch der Physik, Vol. 42, ed. by S. Flügge (Springer-Verlag, Berlin, 1957) p. 556.

9. A few rare earth metals have larger fields (~ 10^7 gauss), and must be excepted from this statement.

10. Hans A. Weidenmüller, Rev. Mod. Phys. 33, 574 (1961).

11. H. W. Taylor and W. R. Frishen, Phys. Rev. 114, 127 (1959).

12. Y. Koi, A. Tsujimura, T. Hihara, and T. Kushida, J. Phys. Soc. Japan 16, 1040 (1961).

13. W. Dobrowolski, R. V. Jones, and C. D. Jeffries, Phys. Rev. 101, 1001 (1955).

14. J. C. Wheatley, D. F. Griffing, and R. D. Hill, Phys. Rev. 99, 334 (1955).

15. R. W. Bauer and M. Deutsch, Phys. Rev. 117, 519 (1960).

16. N. J. Stone and B. G. Turrell, Phys. Letters 1, 39 (1962).

17. J. M. Daniels and N. Kurti, Proc. Roy. Soc. (London) A221, 243 (1954).

18. V. Arp, D. Edmonds, and R. Petersen, Phys. Rev. Letters 3, 212 (1959).

19. R. C. LaForce, private communication to A. M. Portis.

20. E. G. Funk, Jr., and M. L. Wiedenbeck, Phys. Rev. 112, 1247 (1958).

21. B. S. Dzelepov and N. N. Zhurkovsky, Nucl. Phys. 6, 655 (1958).

22. H. W. Taylor and S. A. Scott, Phys. Rev. 114, 121 (1959).

23. A. C. Kuipper, Proc. Phys. Soc. (London) 71, 77 (1958).

24. N. M. Anton'eva, A. A. Bashilov, and E. E. Kulakovskii, Soviet Physics JETP 10, 1063 (1960).

25. Toshio Katsh and Yasukaga Yoshizawa, Nucl. Phys. 32, 5 (1962).

26. T. Suter, P. Reyes-Suter, W. Schever, and E. Aasa, Nucl. Phys. 47, 251 (1963).

27. J. N. Haag, D. A. Shirley, and David H. Templeton, Phys. Rev. 129, 1601 (1963).

28. G. A. Westenbarger and D. A. Shirley, Phys. Rev. 123, 1812 (1961).

29. L. C. Biedenharn and M. E. Rose, Rev. Mod. Phys. 25, 729 (1953).

30. A. J. Dornblatt, Trans. Electrochem. Soc. 74, 280 (1938).

31. Q. O. Navarro, Thesis, University of California, 1962 (UCRL-10362).

32. H. Daniel, O. Mehling, and D. Schotte, Z. Physik 172, 202 (1963).

33. W. B. Ewbank, W. A. Nierenberg, H. A. Shugart, and H. B. Silsbee, Phys. Rev. 110, 595 (1958).

34. O. Ames, A. M. Bernstein, M. H. Brennan, R. A. Haberstroh, and D. R. Hamilton, Phys. Rev. 118, 1599 (1960).

35. O. Ames, A. M. Bernstein, M. H. Brennan, and D. R. Hamilton, Phys. Rev. 123, 1793 (1961).

36. R. K. Girgis and R. van Lieshout, Nucl. Phys. 13, 493 (1959).

Table I. Experimental values of $B_2U_2F_2$ for γ rays from Ag^{110m} nuclei oriented in iron.

Energy,[a] keV	Relative intensity,[b] with errors in parentheses	$B_2U_2F_2$ at 0.111° K (errors in parentheses)
447	6.4 (0.8)	< 0
620	3.9 (0.5)	> - 0.3
658	100	< - 0.215[c]
677	10 (1)	> 0
687	7 (1)	
706	19 (2)	> + 0.30
744	6 (2)	----
764	24 (2)	- 0.30 (2)
818	8.5 (1)	----
885	76 (4)	- 0.324
937	33 (2)	- 0.31 (1)
1384	27 (2)	+ 0.680 (10)
1476	5.5 (1)	+ 0.480 (6)
1505	14 (1)	
1561	1.3 (0.2)	

[a] From Refs. 25 and 26.

[b] From Refs. 21 and 24.

[c] The value - 0.215 includes contributions from the 620, 677, and 687 keV transitions.

Table II. Angular distribution coefficients and derived amplitude mixing ratios for the 1384 keV γ ray in Cd^{110}.

F_2[a]	Type[b]	δ (E2/M1)[a,c]	Ref.
+ 0.74 (5)	L	- 0.274 (34)	this work
+ 0.634 (16)	F	+ 0.341 (12)	11
+ 0.688 (29)	F	+ 0.387 (30)	20
+ 0.643 (27)	F	+ 0.349 (22)	23

[a] Errors in last place are given in parentheses.

[b] The "first" and "last" in cascade classification is discussed in Ref. 28.

[c] By definition, $\delta^F = - \delta^L$.

Table III. Angular distribution coefficients and derived amplitude mixing ratios for the 1505 keV γ ray in Cd^{110}.

Observed Function[a]	Value (errors in parentheses)	Derived F_2[b]	$\delta(\frac{E2}{M1})$	Reference
$U_2F_2(1505)$	+0.506(25)	+1.06(10)	$-0.43 > \delta^L > -1.32$	this work
$A_2(764\text{-}1505)$	-0.1627(63)	+1.03(6)	$-0.44 > \delta^L > -1.29$	11
$A_2(1505\text{-}658)$	-0.34(7)	+0.63(13)	$+0.31 < \delta^F < +0.59$	23
$A_2(1505\text{-}658)$	$-0.40\ ^{+0.13}_{-0.07}$	+0.78(18)	$+0.41 < \delta^F < +4.6$	20

Value adopted from overlap of allowed ranges: $\delta^L = -.515(75)$.

[a] The measurements were made on the "1505 keV peak," which includes much of the 1476 and 1561 keV γ rays.

[b] Corrections have been made for interfering radiations, as discussed in text.

FIGURE CAPTIONS

Figure 1. Warm-up curve for chrome-alum slurry and fin assembly. The maximum susceptibility occurs just below the Curie temperature. Note that after 3.8 hr the slurry has warmed up only to a $1/T^*$ of 23. This corresponds to an absolute temperature of 0.02° K.

Figure 2. Plot of alloy temperature against magnetic temperature of salt slurry. Solid curve is the salt temperature, based on the $T\text{-}T^*$ correlation. Three sets of points give temperature obtained from Co^{60} thermometer in three different assemblies.

Figure 3. Magnitude of $W(0)$ for Co^{60} in iron as a function of time after end of demagnetization. This run was used for Fig. 1 and data from it appear as shaded rectangles in Fig. 2.

Figure 4. Decay scheme of Ag^{110m}.

Figure 5. Gamma-ray spectrum of Ag^{110m} obtained along polarizing axis with the iron alloy cooled to near 0.01°K (dashed curve) and about 1°K (solid curve).

Figure 6. Plot of $W(0)$ vs photon energy for Ag^{110m} nuclei oriented at 10^{-2} $^\circ$K in iron. Several unresolved γ-rays are clearly aniostropic.

Figure 7. Average value of B_2 obtained by analysis of three γ rays from Ag^{110m} in iron plotted as a function of $1/T$. The curves were calculated by using the values of $|\mu H|$ shown. The curves are (from the top) for $|\mu H|$ of 1.1×10^6, 1.0×10^6, and 0.9×10^6 nm gauss, respectively.

Figure 8. Average value of B_2 obtained by analysis of three γ rays from Ag^{110m} in nickel plotted as a function of $1/T$. The curves were calculated by using the values of μH shown.

Figure 9. Experimental $B_4U_4F_4(885)$ for Ag^{110m} in iron vs 1/T. Curves calculated for values of μH of (from top) 1.1, 1.0, and 0.9×10^6 nm gauss are shown.

Figure 10. Beta intensity from Ag^{110m} nuclei polarized in iron at 0.01°K, taken with and against the polarizing field, and normalizing intensity for randomly oriented nuclei at 1°K. For this 6+ to 6+ decay electrons are emitted preferentially in the direction away from the angular momentum vector. Enhancement of intensity along external field direction indicates that nuclei are oriented against this field. No energy scale is given because an accurate calibration was impossible, but this is the 400 keV region and consists almost entirely of the 530-keV branch.

Figure 11. Beta intensity from Ag^{110m} nuclei polarized in nickel at 0.01°K, with normalized intensity, as in Fig. 10.

Figure 12. Partial decay scheme for Ag^{104}, after Ref. 36.

Figure 13. Gamma-ray spectrum of Ag^{104} polarized in iron. Spectra obtained parallel and perpendicular to axis of polarization are shown. Solid curves are isotropic spectra normalized to cold counting period. Dashed curves are for $1/T \approx 60$.

Figure 14. W(0)-1 for 920-keV γ ray from Ag^{104} as function of temperture. Two extreme values are shown at each temperature. Curves are for various values of the hyperfine field.

Figure 15. Positron counting rate as function of time after demagnetization. Note that $W(0) < 1$ and $W(\pi) > 1$ for positrons, indicating a negative hyperfine field.

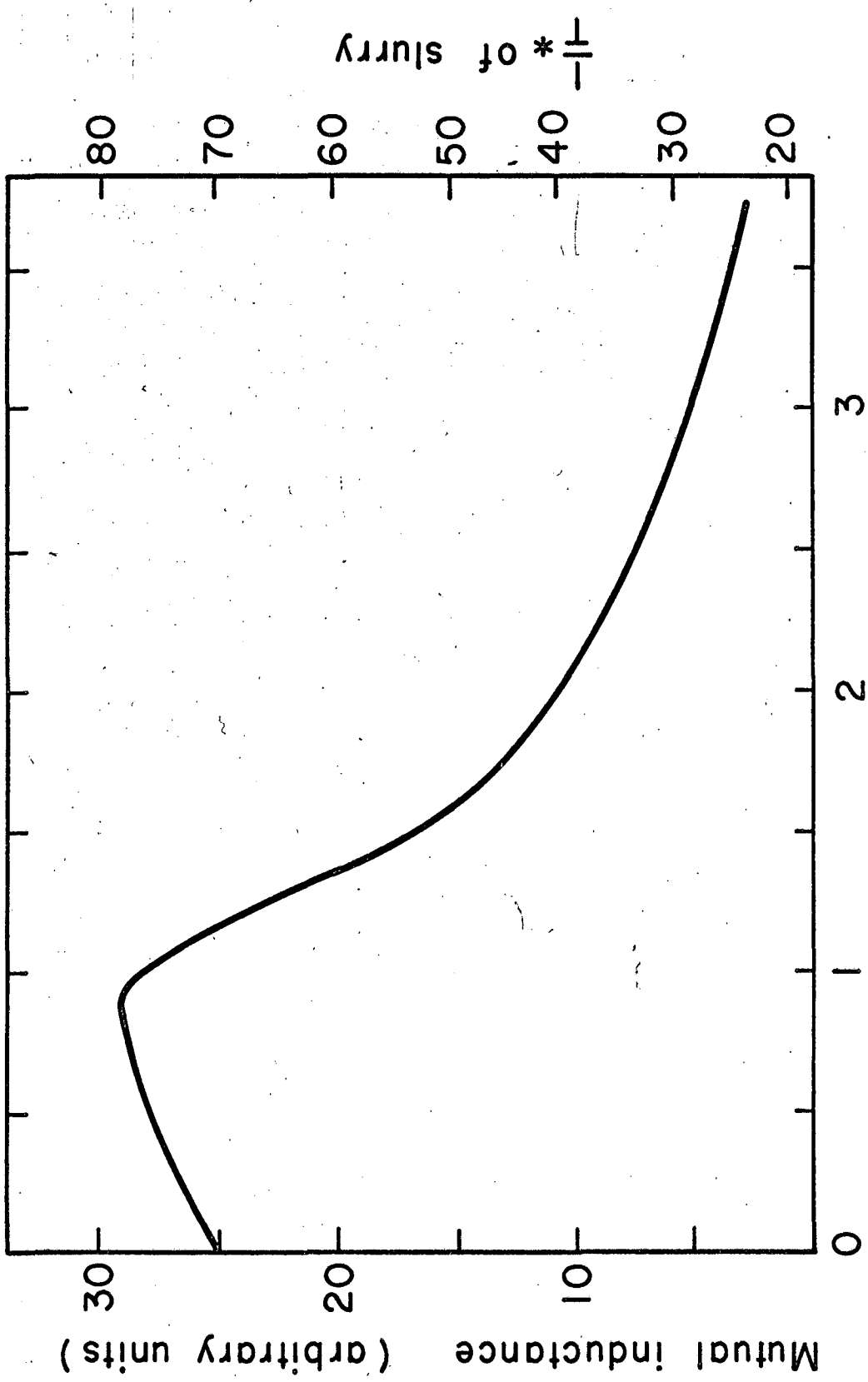
MU-32934
Mutual inductance (arbitrary units)
30
20
10
0
1
2
3
Time (hr)
80
70
60
50
40
30
20
1/τ * of slurry

Fig. 1

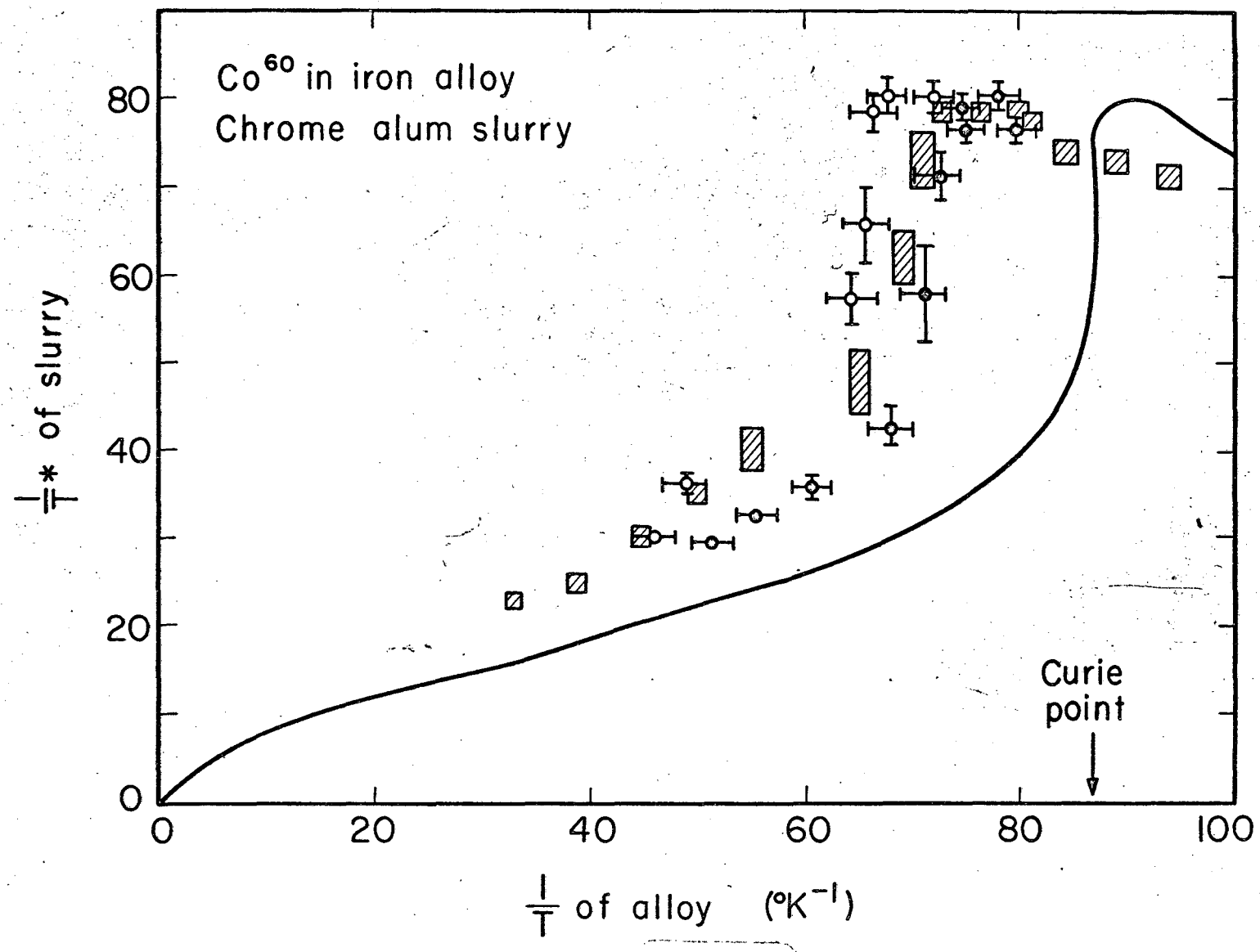
Co60 in iron alloy
Chrome alum slurry
1/T* of slurry
1/T of alloy (°K⁻¹)
Curie point
0
20
40
60
80
100
MU-32935

Fig. 2

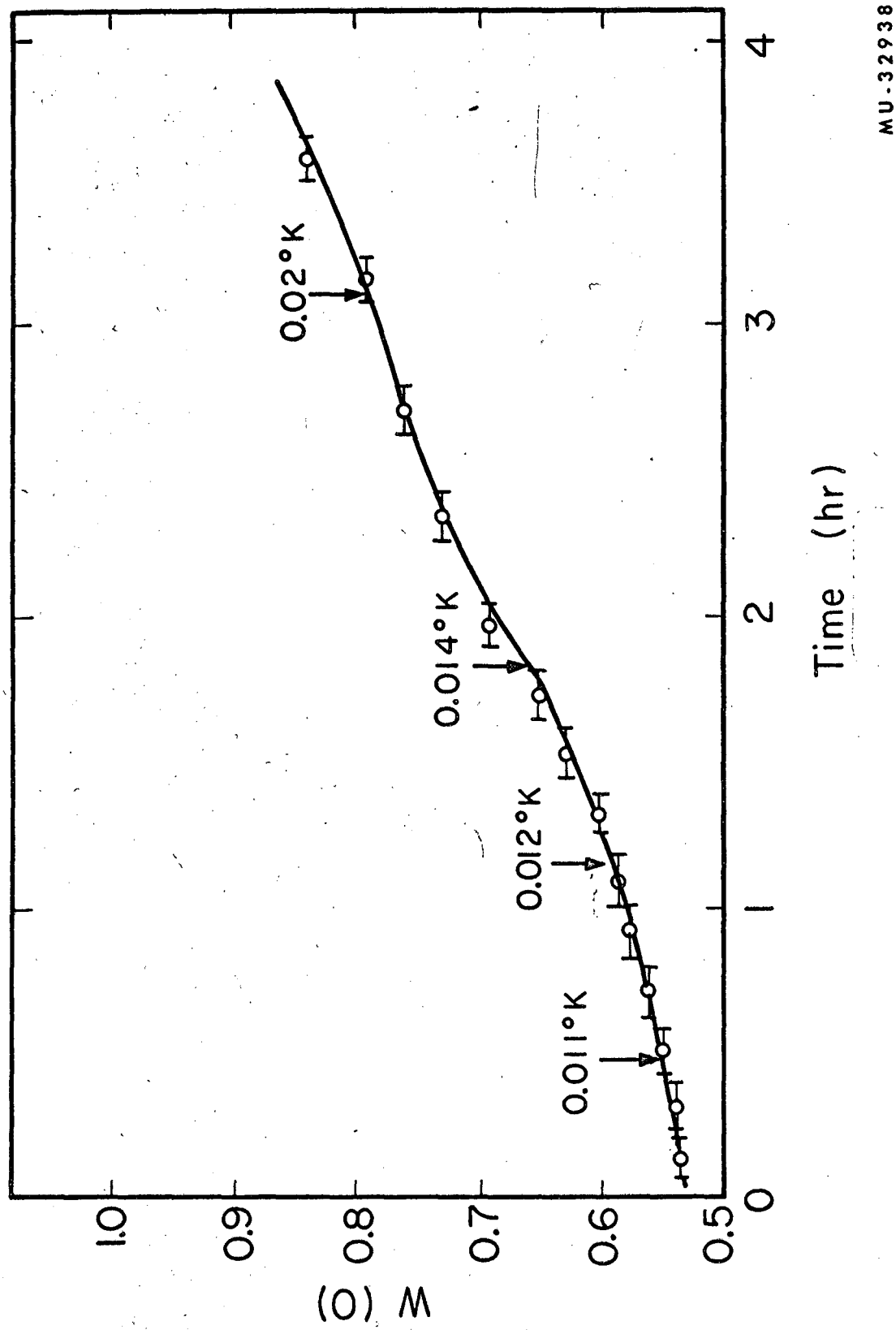
W (0)
1.0
0.9
0.8
0.7
0.6
0.5
0
1
2
3
4
Time (hr)
0.02°K
0.014°K
0.012°K
0.011°K
MU-32938

Fig. 3

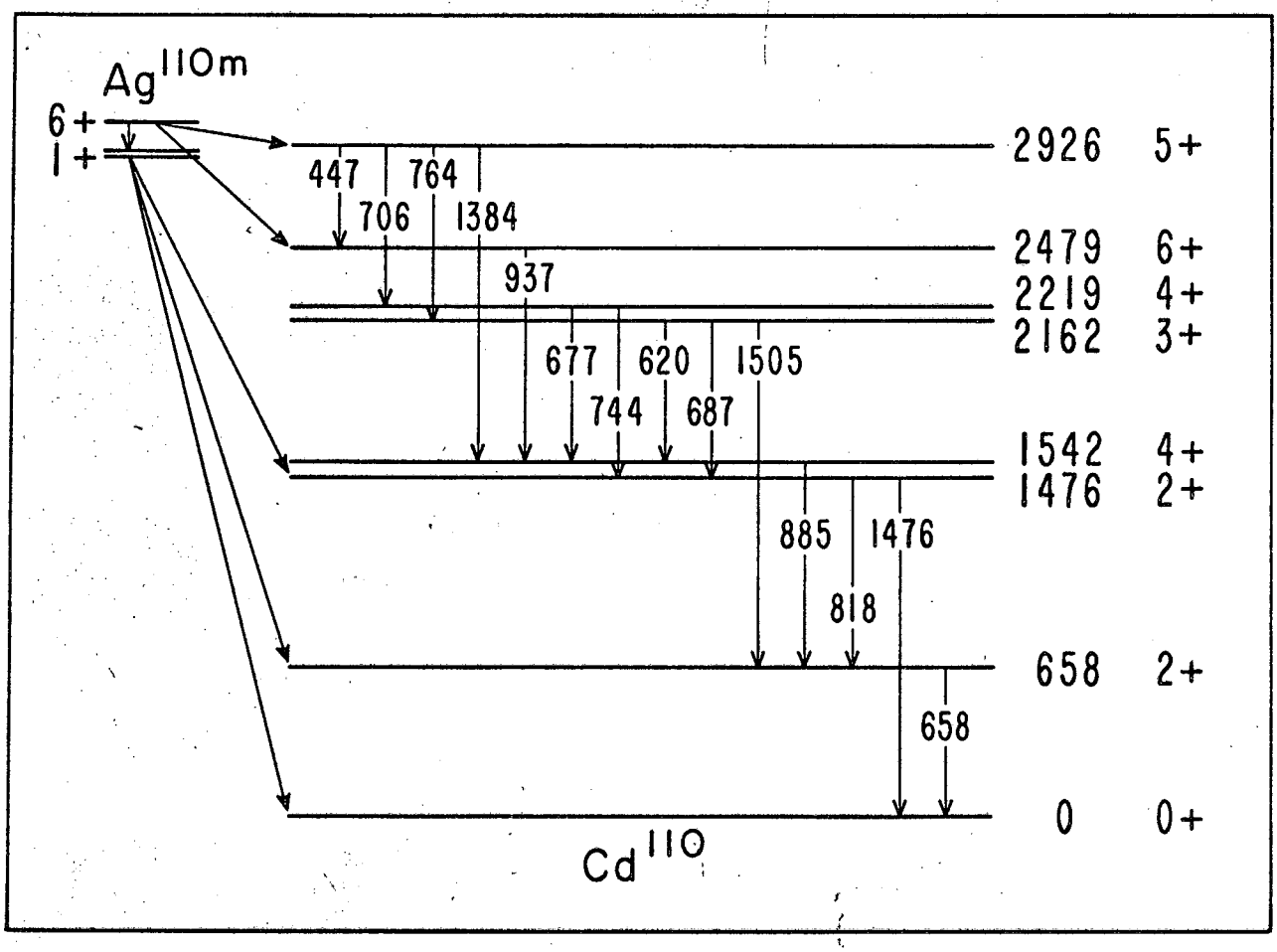

MUB-4055

Fig. 4

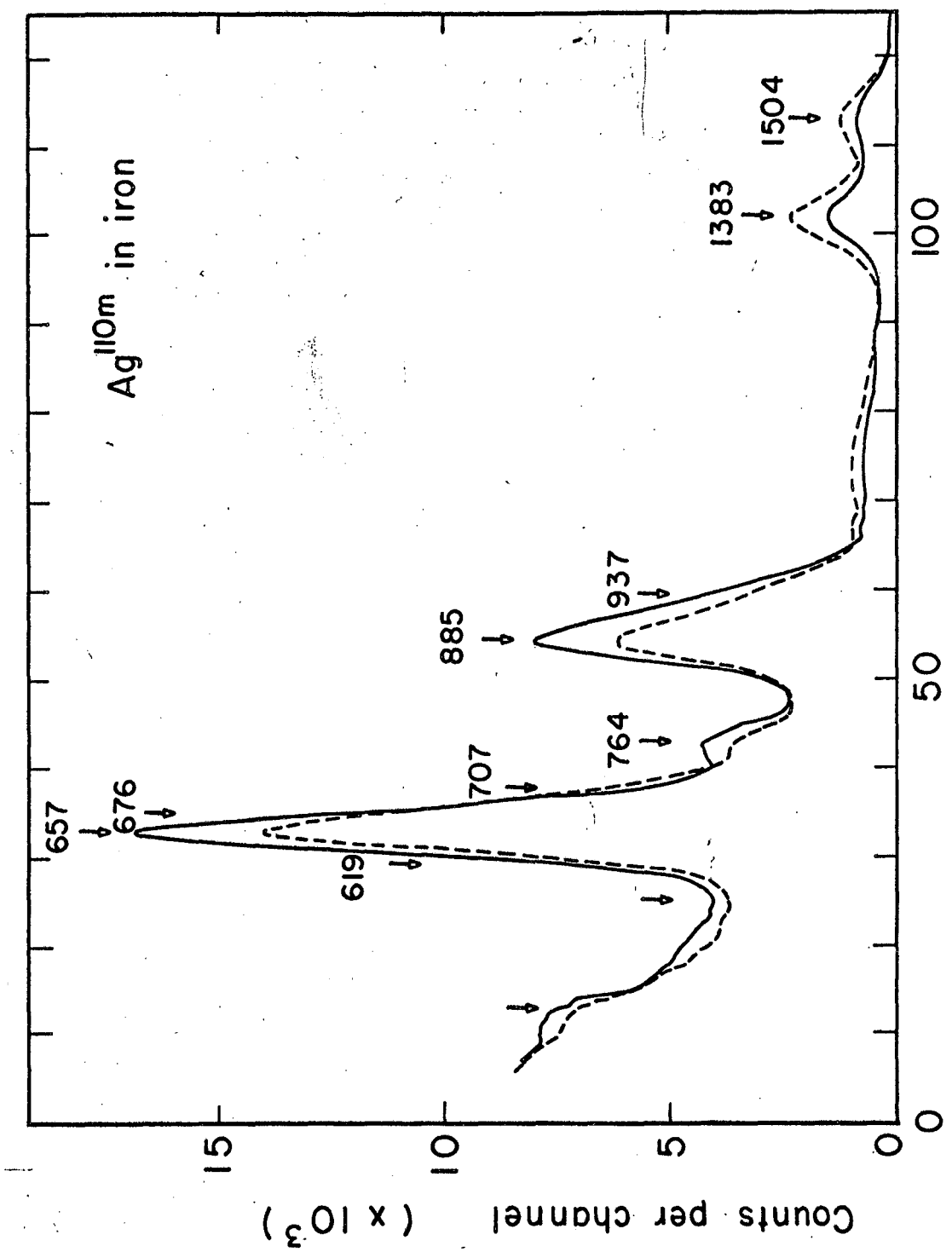

MU-32940

Fig. 5

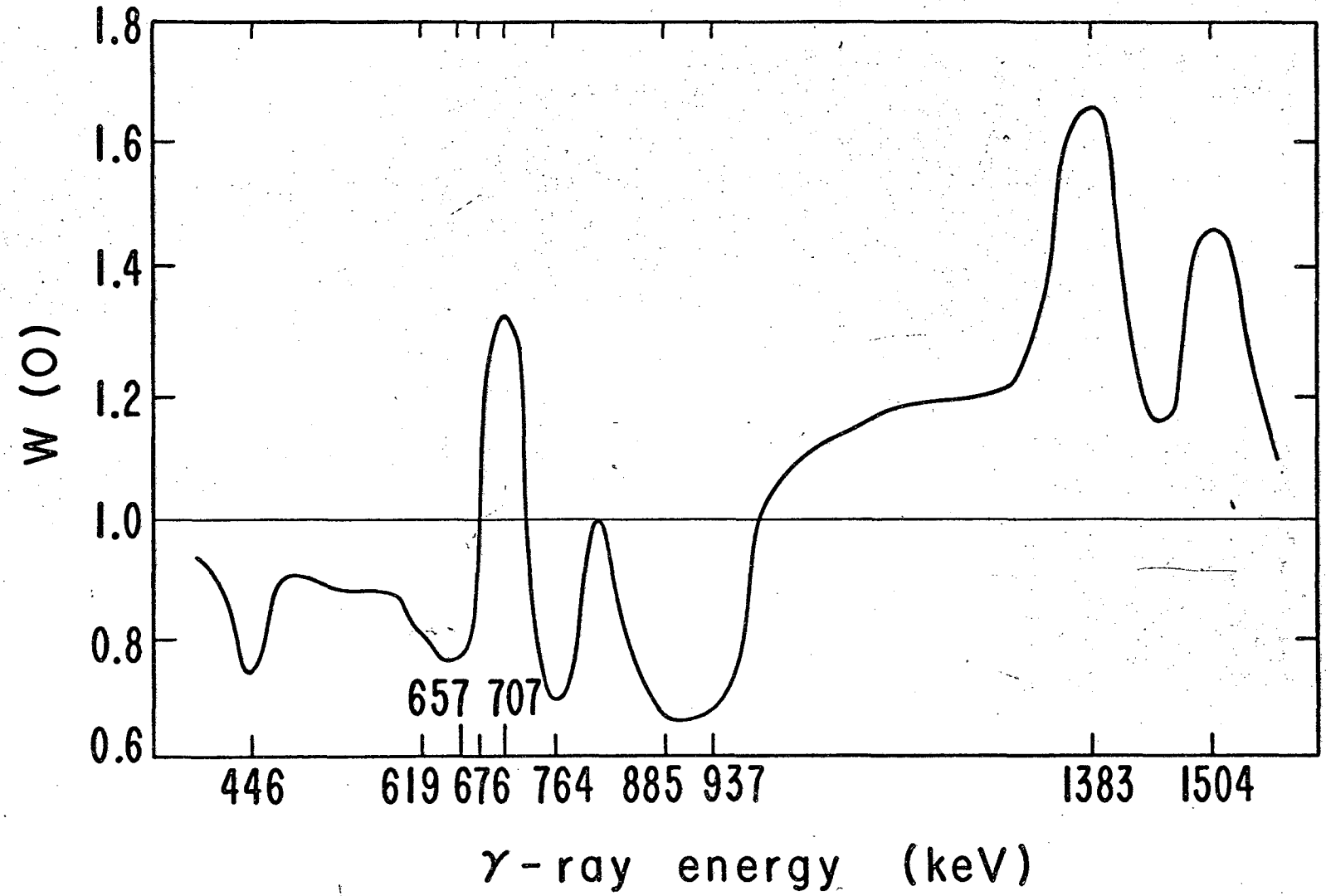

MU-32941

Fig. 6

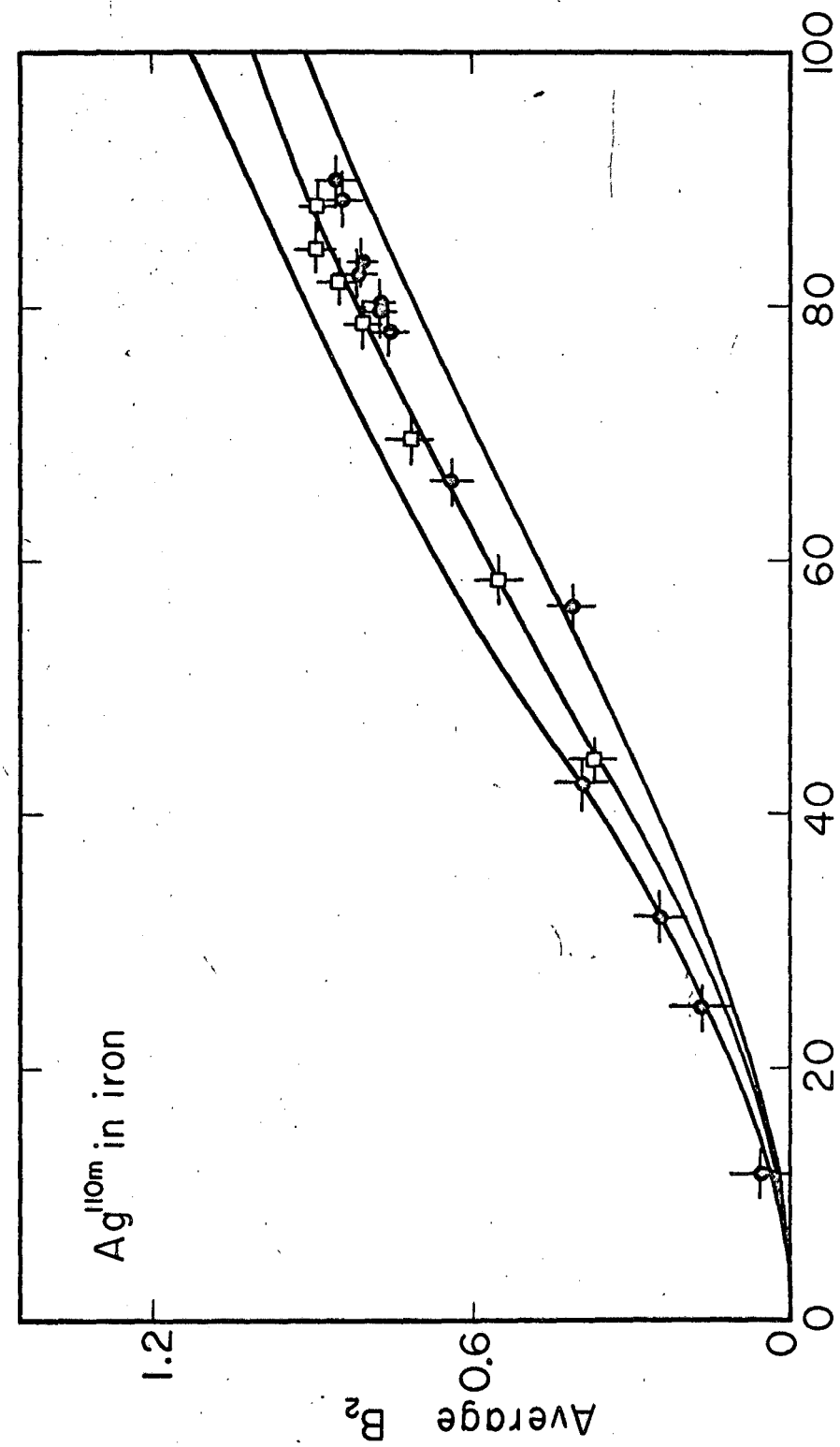

MU-32943

Fig. 7

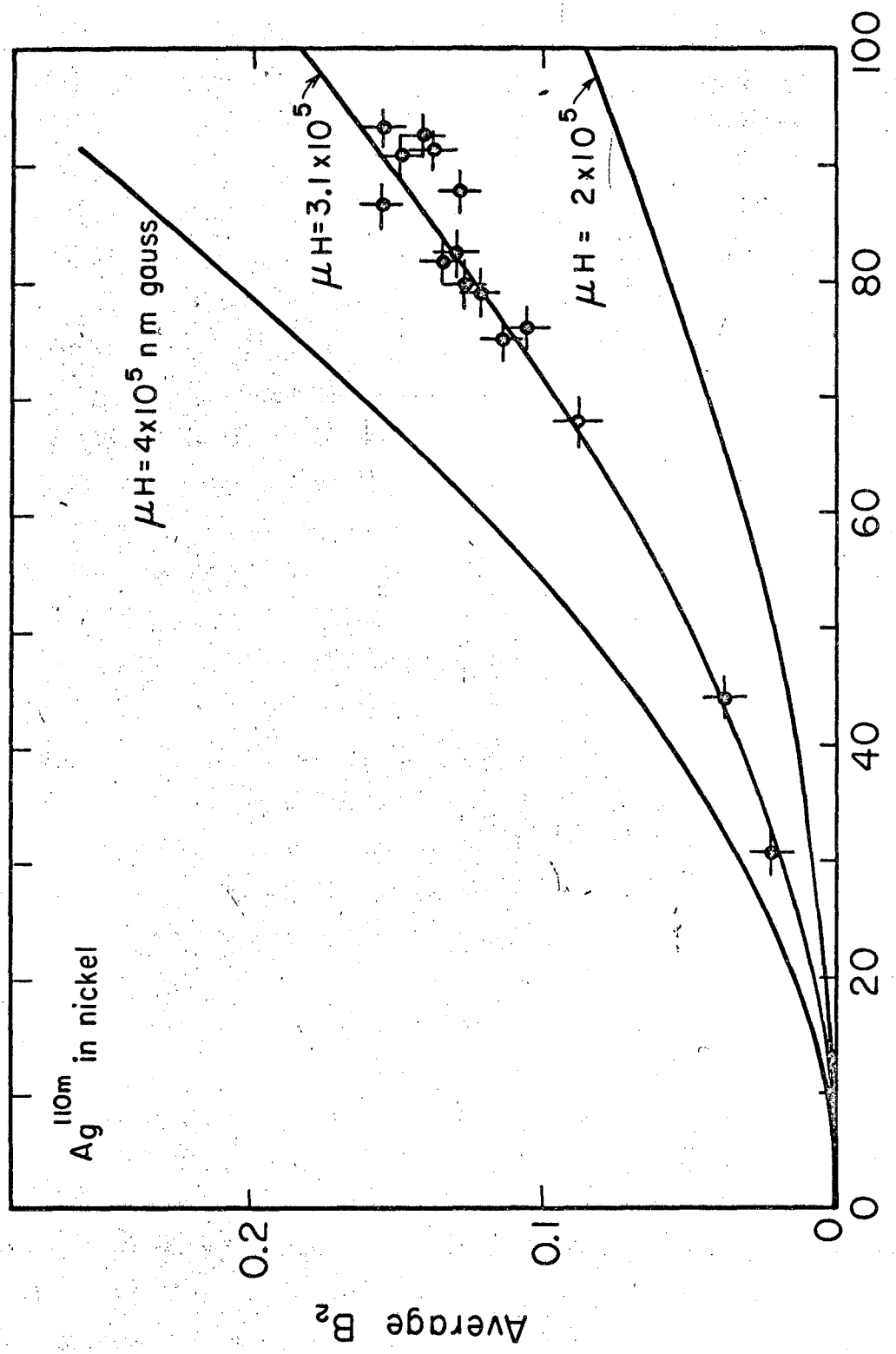
Average B_2
0.2
0.1
0
0
20
40
60
80
100
$\frac{1}{T}$ ($^\circ K^{-1}$)
Ag^{110m} in nickel
$\mu H = 4 \times 10^5$ n m gauss
$\mu H = 3.1 \times 10^5$
$\mu H = 2 \times 10^5$
MU-32949

Fig. 8

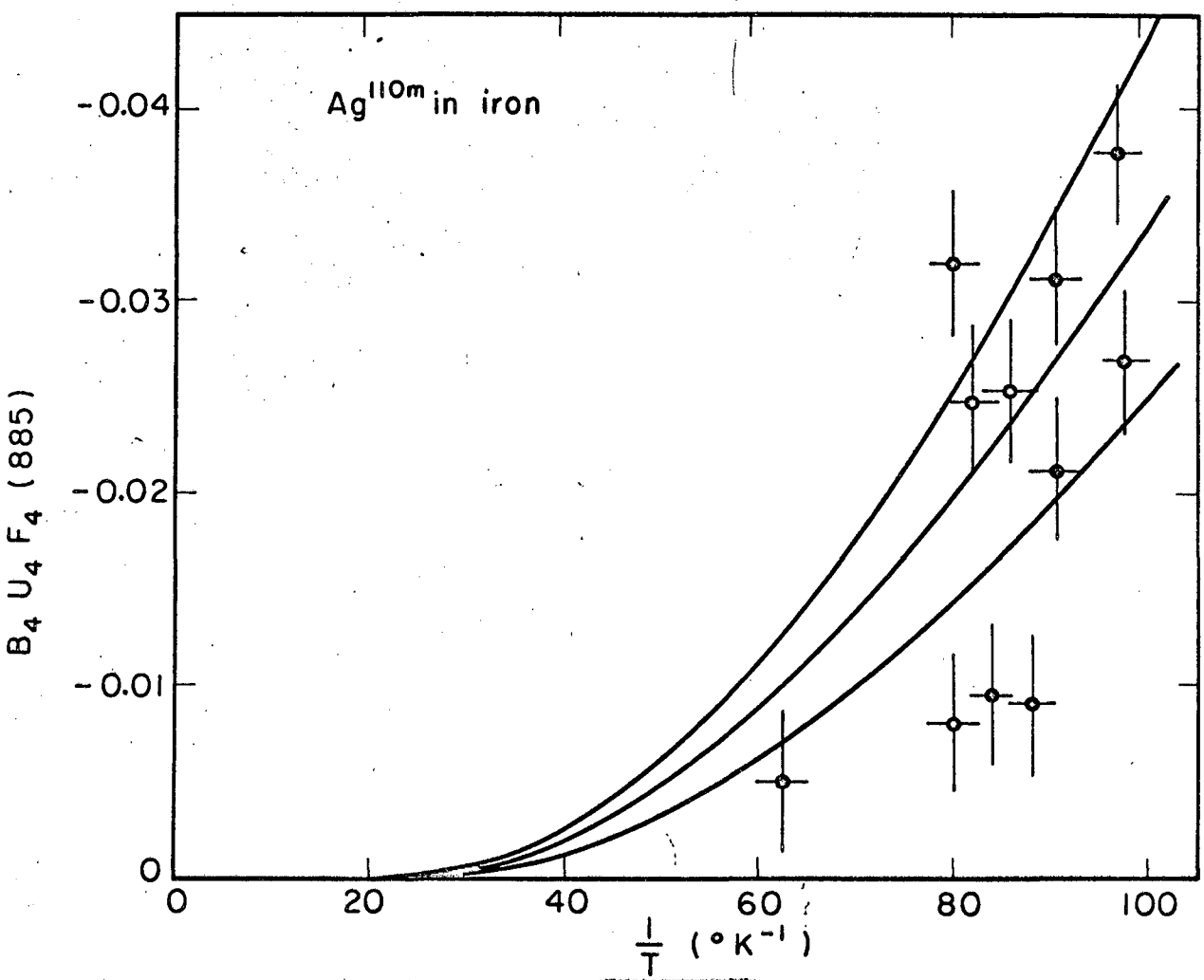

MUB-4056

Fig. 9

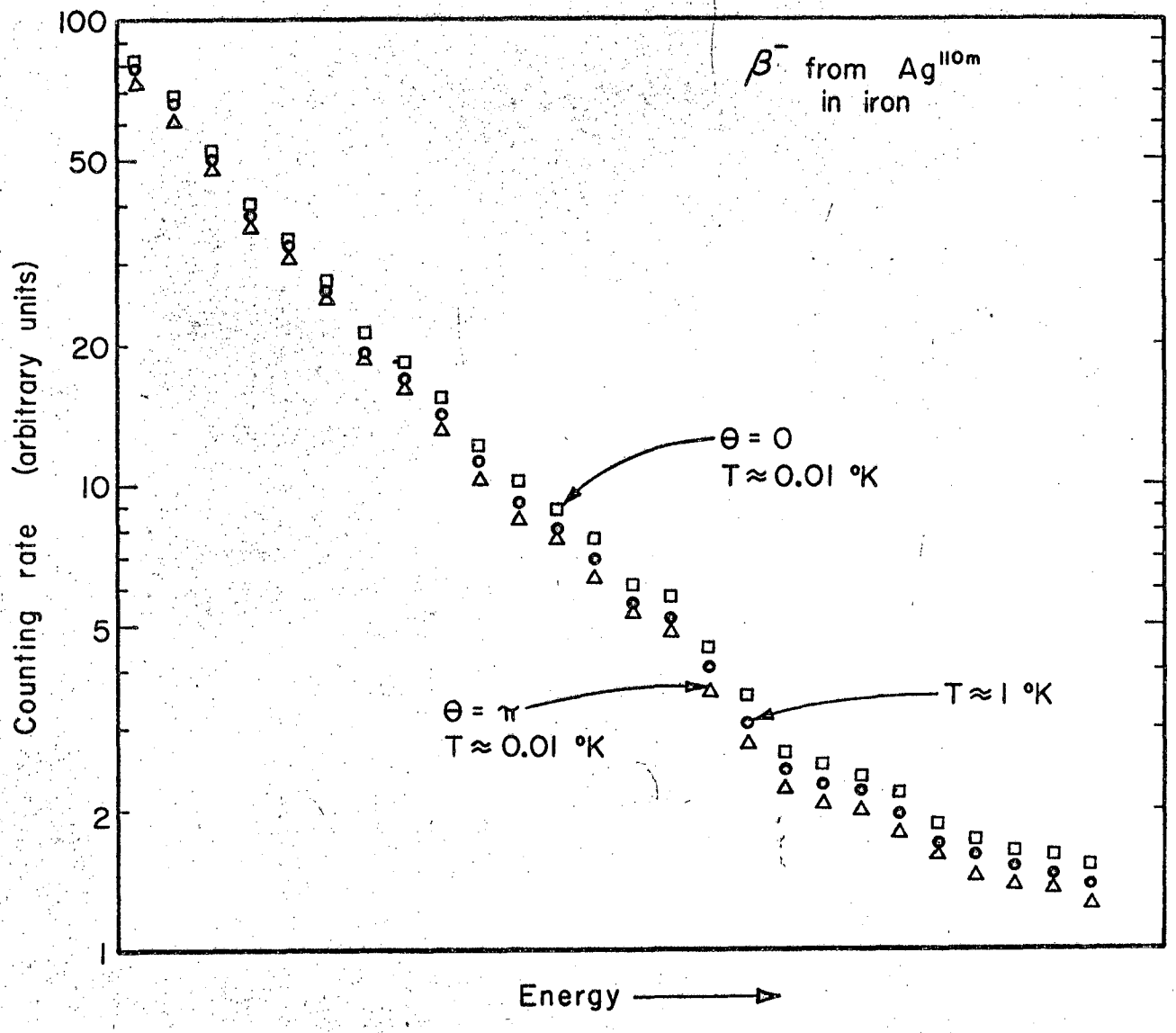
β⁻ from Ag^110m
in iron
Counting rate (arbitrary units)
100
50
20
10
5
2
1
θ = 0
T ≈ 0.01 °K
θ = π
T ≈ 0.01 °K
T ≈ 1 °K
Energy
MUB-4057

Fig. 10

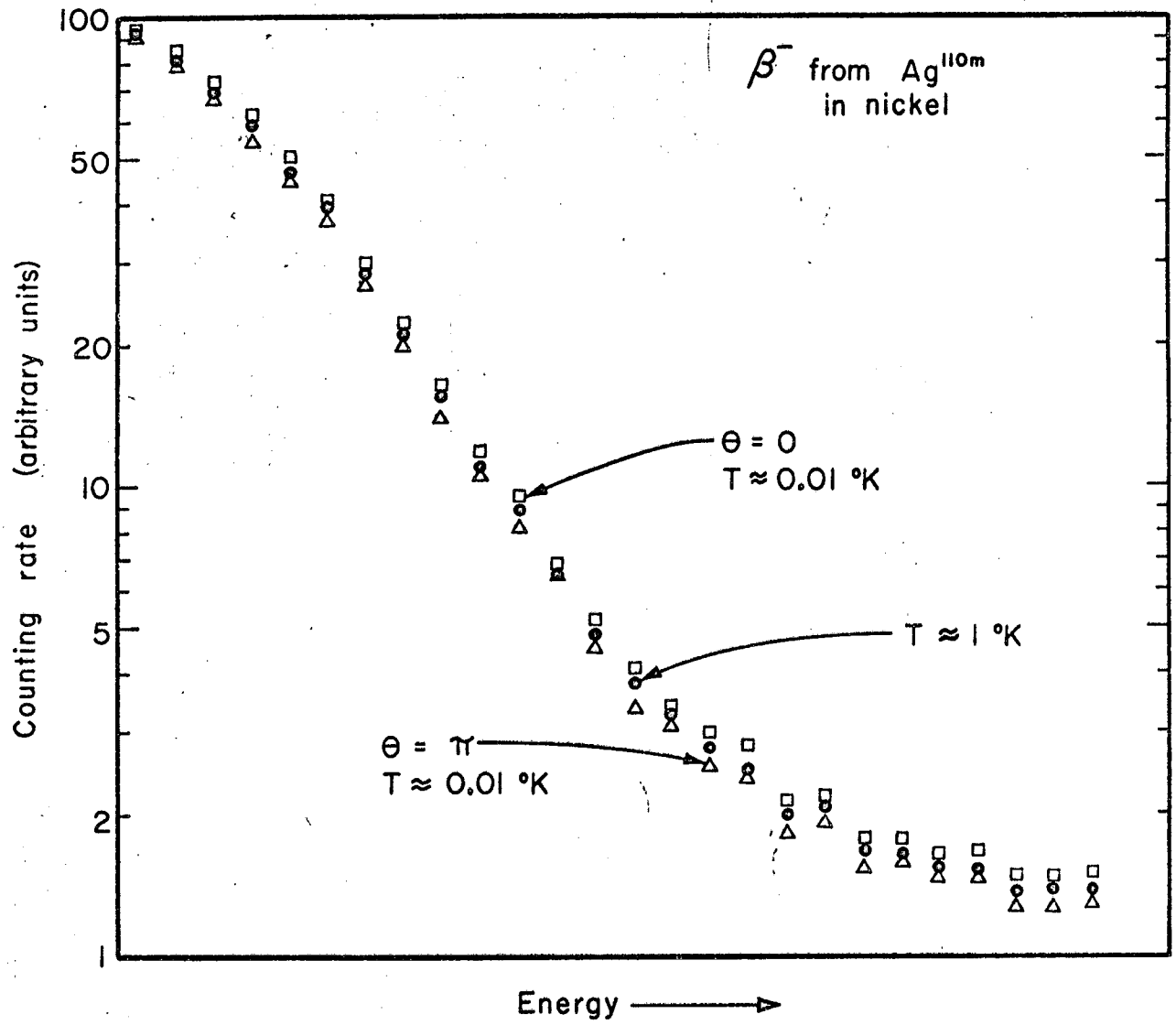

MUB-4058

Fig. 11

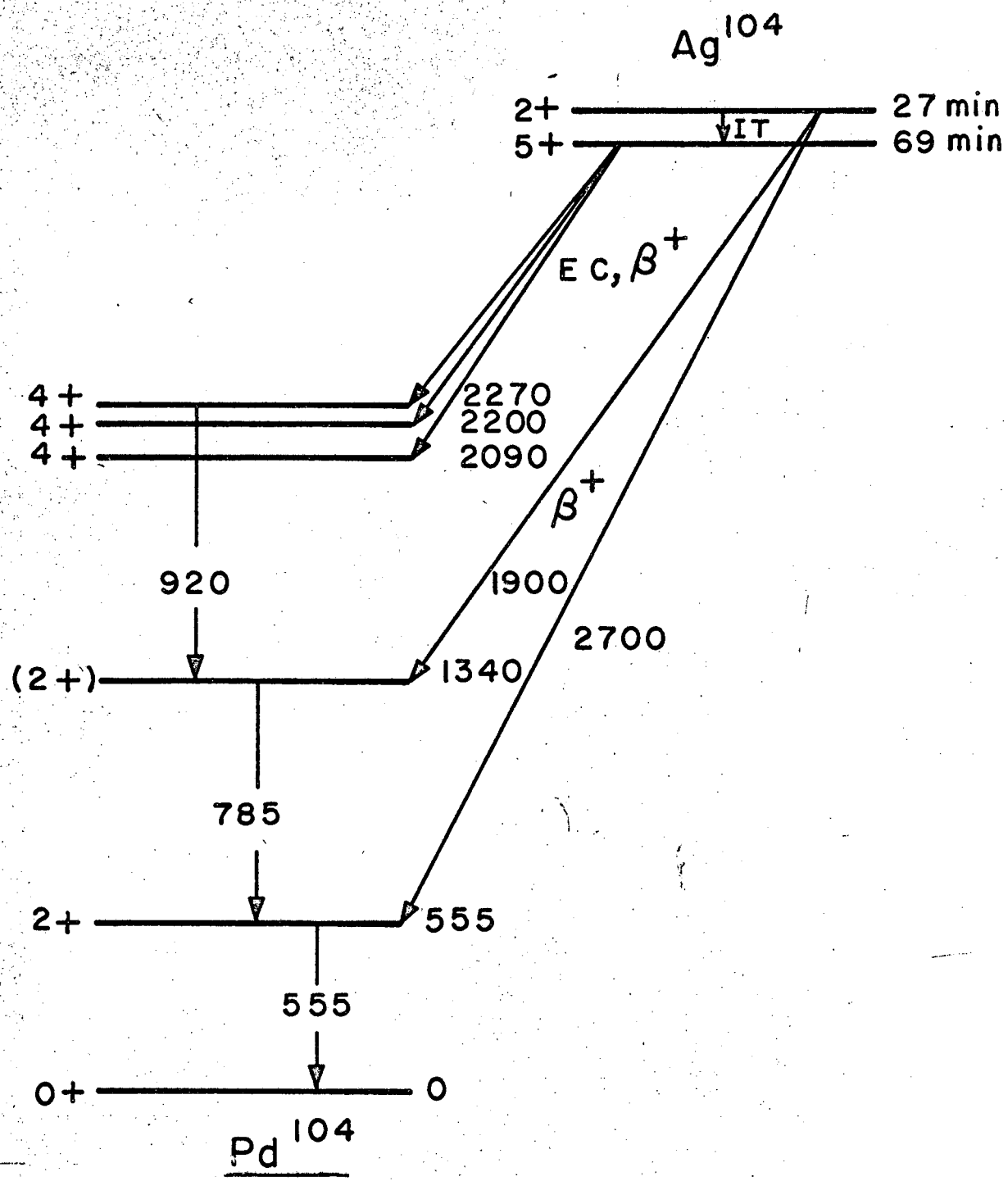

Fig. 12

MU-32958

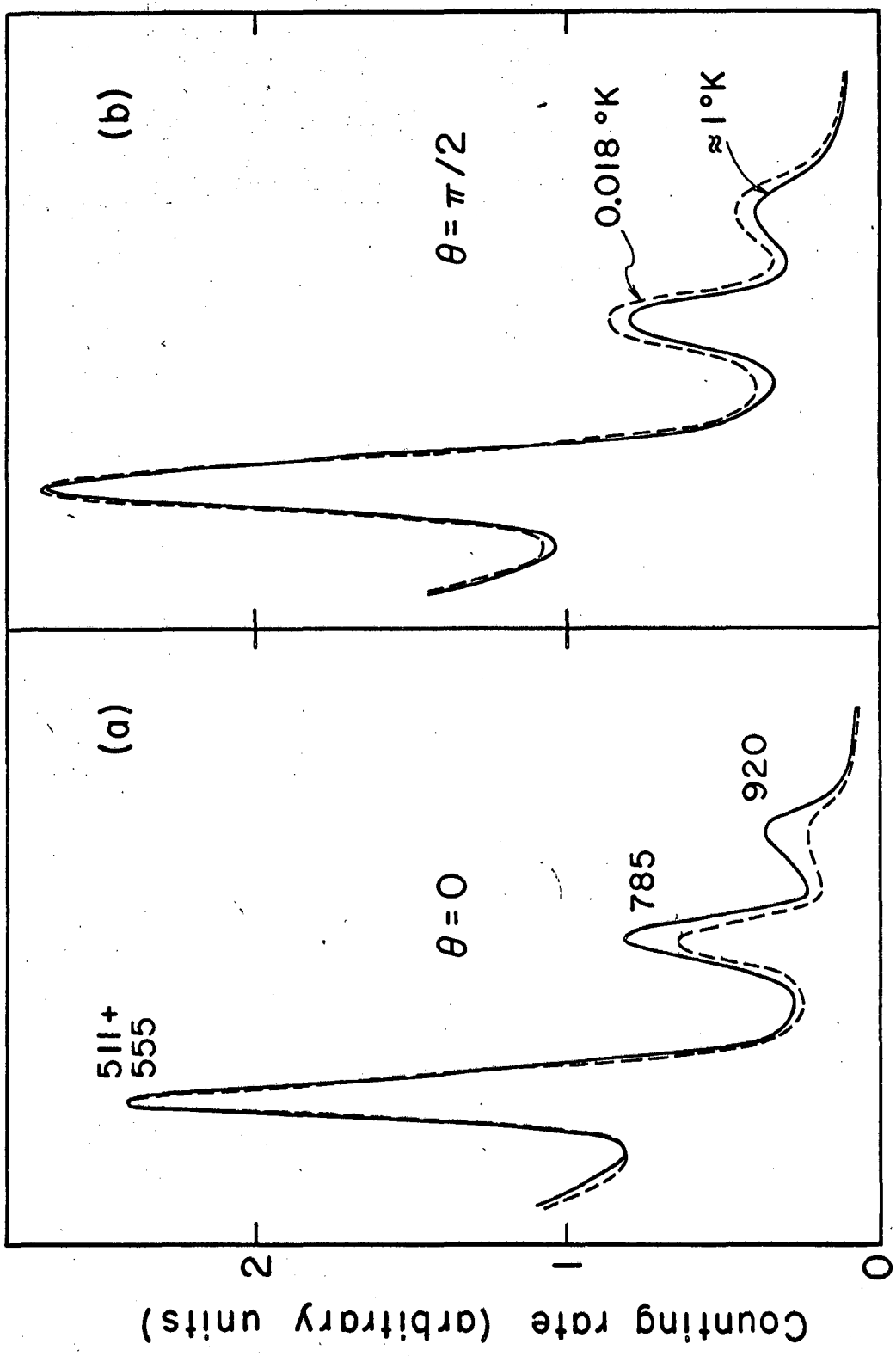

MU-32959

Fig. 13

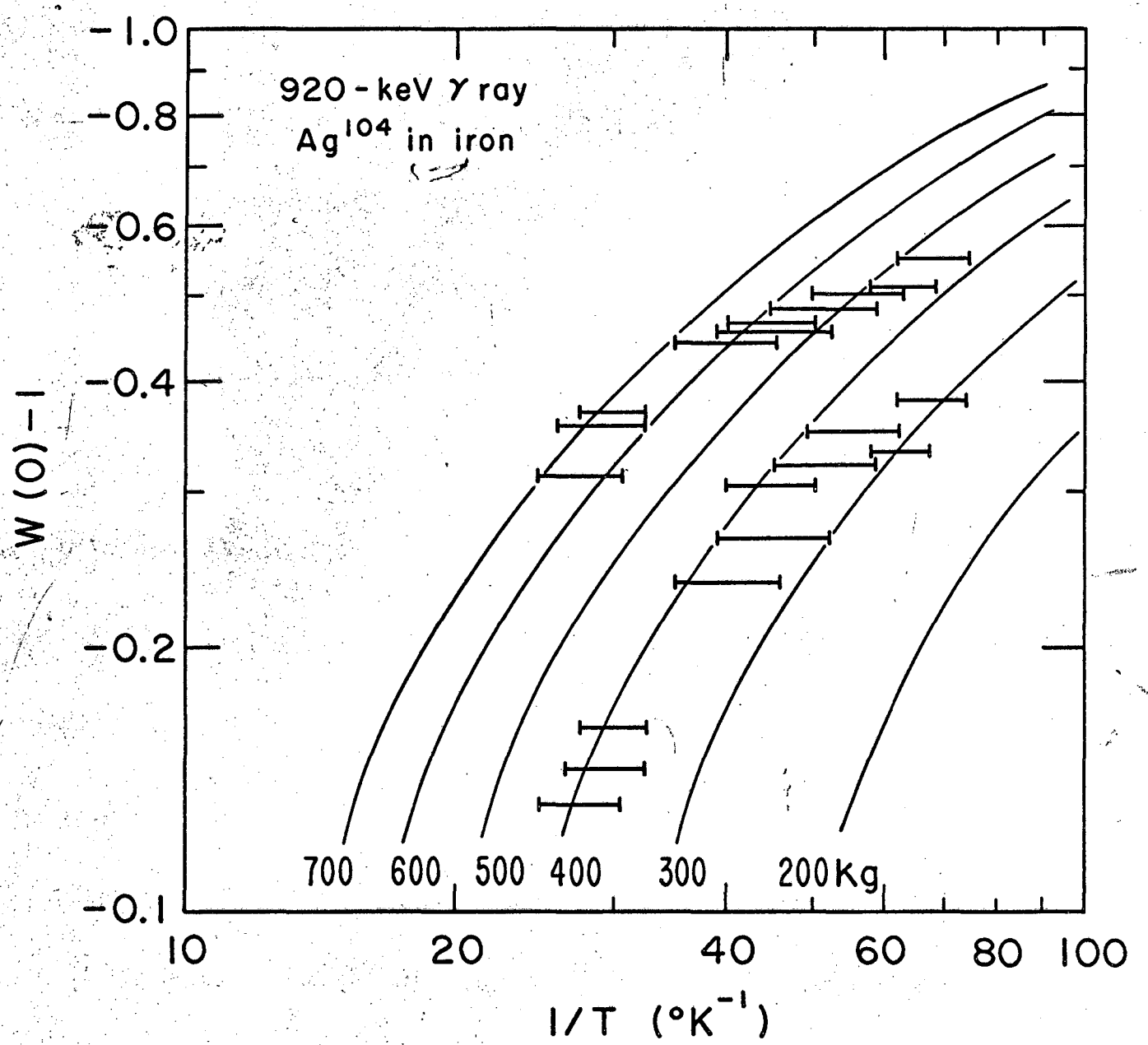

MU-32960

Fig. 14

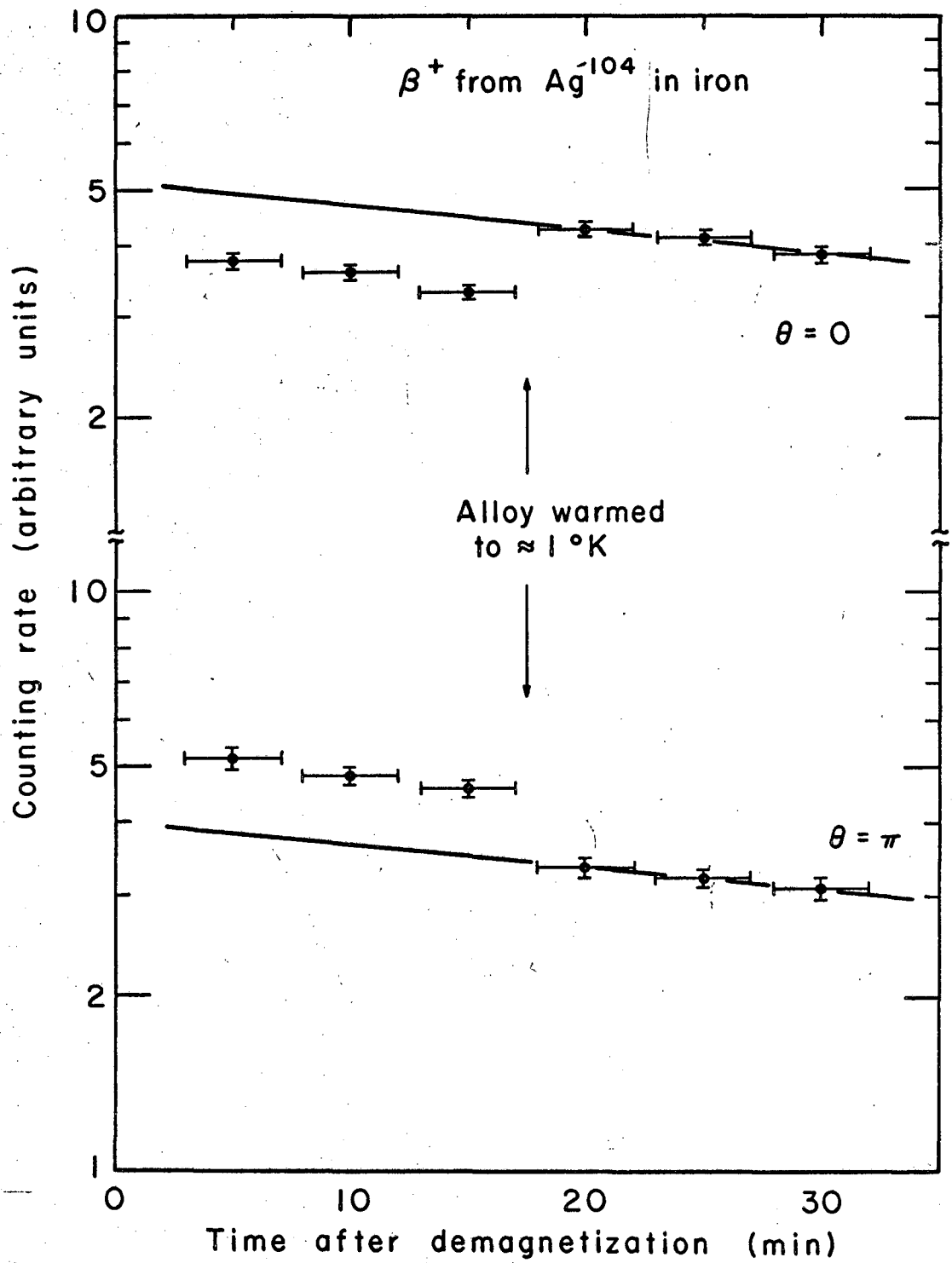

MU-32962

Fig. 15